

Uncertainty-Aware Active Source Tracking of Marine Pollution using Unmanned Surface Vehicles

Song Ma¹, Richard Bucknall¹ and Yuanchang Liu¹

Abstract—This paper proposes an uncertainty-aware marine pollution source tracking framework for unmanned surface vehicles (USVs). By integrating high-fidelity marine pollution dispersion simulation with informative path planning techniques, we demonstrate effective identification of pollution sources in marine environments. The proposed approach is implemented based on Robot Operating System (ROS), processing real-time sensor data to update probabilistic source location estimates. The system progressively refines the estimation of source location while quantifying uncertainty levels in its predictions. Experiments conducted in simulated environments with varying source locations, flow conditions, and starting positions demonstrate the framework’s ability to localise pollution sources with high accuracy. Results show that the proposed approach achieves reliable source localisation efficiently. This work contributes to the development of full autonomous environmental monitoring capabilities essential for rapid response to marine pollution incidents.

Index Terms—marine robotics, informative path planning, environmental monitoring, decision making, unmanned surface vehicle

I. INTRODUCTION

Pollution discharged into the marine environment causes severe consequences to ecosystems [1], [2] and human health [3]. The marine pollution problem is a result of various reasons. According to Biswas et al. [4], coastal waters are endangered by sewerage discharge, agricultural, and industrial waste. Even in the far seas, water bodies also face hazards like oil spills and chemical leaks from various maritime activities [5]. To minimise the influence of marine pollution, reliable monitoring and rapid responses play a crucial role.

In order to better monitor marine pollution and restrict its influence, the use of robotics systems has attracted much attention, which reduces the risks that humans are exposed to [6]. In particular, the use of robotic systems in environmental monitoring has been widely investigated [7], and it demonstrates significantly higher efficiency compared with conventional solutions [8]. A crucial sub-problem within robotic marine monitoring is the task of localising the pollution source, often referred to as source tracking [9].

Early approaches to pollution source tracking focused on establishing estimation models of the source locations. For example, Pang and Farrel [10] used Bayesian inference to generate a probability map of the source location in a marine

This work was supported by the Dean’s Prize of UCL Engineering; the China Scholarship Council; Engineering and Physical Sciences Research Council (EPSRC) [grant number EP/Y000862/1].

¹ Department of Mechanical Engineering, University College London, Torrington Place, London, WC1E 7JE, the United Kingdom. {song.ma.18, r.bucknall, yuanchang.liu}@ucl.ac.uk

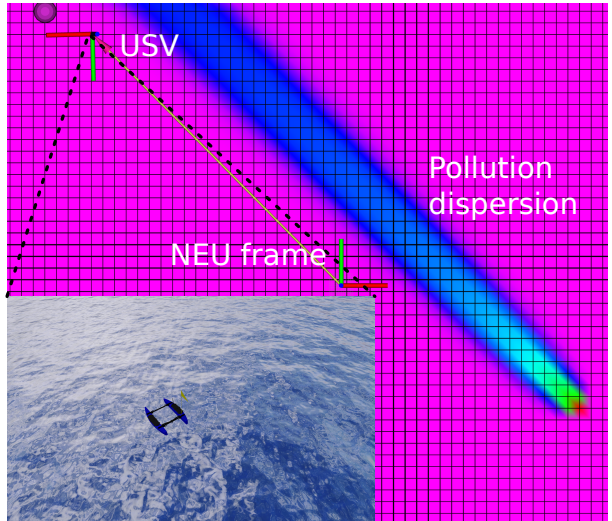


Fig. 1: Survey USV cruising in high-fidelity simulated environment, searching for pollution source.

environment, while Hutchinson et al. [11] applied a similar principle to airborne source localisation using a particle filter. A key limitation of these methods is their reliance on external control inputs, such as a predefined search pattern (e.g., a lawnmower pattern), to collect data. Consequently, these methods are not fully autonomous and can be considered as a variant of deploying a fixed sensor network [12].

To overcome this reliance on predefined paths and achieve full autonomy, research has shifted towards active control strategies, often referred to as active information gathering or Informative Path Planning (IPP) [13]. Several researchers have proposed to incorporate the IPP to substitute the external control in the fields of localisation [14], Simultaneous Localisation and Mapping (SLAM) [15], and 3D reconstruction [16]. However, little attention has been paid to the active marine pollution source tracking. A limited number of existing cases [17], [18] applied IPP for gas source localisation, but the scenarios were restricted to indoor applications where their scales were considerably smaller than in the marine environment. Although Bayat et al. [19] put forward active source tracking for marine pollution, the simulated validation was over-simplistic, and their investigated method for estimating the source location in Bayat et al. [19] was restricted to particle filters. Further study in active source tracking in the marine environment using Bayesian-based estimation and the associated validations based on high-fidelity simulations are

necessary.

In the present paper, an uncertainty-aware active pollution source tracking framework using Bayesian estimation is proposed. The proposed framework can be fully integrated into a carefully constructed high-fidelity marine pollution simulator, as shown in Fig. 1.

II. ACTIVE SOURCE TRACKING FRAMEWORK

The proposed framework consists of two modules: (1) a high-fidelity simulator for both marine pollution and the survey Unmanned Surface Vehicle (USV); (2) a Robot Operating System (ROS)-based source tracking system navigating the survey USV through sending waypoints to the ArduPilot interface, as can be seen from Fig. 2. Such a simulation-driven framework plays a significant role in the development and validation processes of robotic software, as it allows for extensive testing without the need for physical hardware. This is particularly important in the context of marine pollution monitoring, where hardware testing can be challenging and expensive. The source tracking algorithm was wrapped as ROS packages, which enables an efficient switch from simulations to hardware implementations.

The simulator module includes two parts. First, a Computational Fluid Dynamics (CFD) solver is used to compute and simulate the dispersion of the pollutant based on source input, $f(p)$, the initial concentration, c_0 , and the wave velocity, \mathbf{v} . Second, a physical simulator of the survey USV is used to process the control input and derive the hydrodynamic response of the USV.

The dispersion of the pollutant is modelled by the diffusion-advection equation as reported previously in our work [20]. The diffusion-advection model has been used in numerous investigations [21], [22] related to environmental monitoring. The diffusion-advection equation is given as:

$$\dot{c}(p, t) - \lambda \nabla^2 c(p, t) + \nabla \cdot (\mathbf{v} c(p, t)) = f(p) \quad (1)$$

where $c(p, t)$ is the spatio-temporal scalar field describing the concentration of the dispersion; λ is the diffusion coefficient; \mathbf{v} is the wave velocity; $f(p)$ is the source input. As mentioned above, given the initial concentration, c_0 , source input, $f(p)$, and the wave velocity, \mathbf{v} , the pollutant concentration distributed in the spatial area, over time, can be quantified by solving the equation. This procedure can be calculated using common CFD solvers. In this work, we adopted the reliable open-source solution from OpenFOAM [23], which is one of the best-known CFD solvers. An example of the simulated pollutant dispersion is shown in Fig. 3.

The physical simulator of the survey USV is mainly based on the Gazebo simulator. This allows easy integration with a rich selection of open-source libraries. In this work, the implementation of a wave-driven USV hydrodynamics simulator [24], and ArduPilot, the autopilot software [25], are utilised. The hydrodynamics simulator allows for an exceptionally high-fidelity environment. In this simulated environment, the consistency between the hydrodynamics of the USV and the pollutant advection is rigorously facilitated by aligning the

wave velocity parameters in both the CFD solver and the physical simulator. What is more, the ArduPilot is used to generate thruster commands based on the higher-level navigation waypoints. This allows for the integration of navigation and control systems, enabling the USV to autonomously follow waypoints and perform complex manoeuvres.

In this work, the data interfaces between the simulator module and the ROS-based source tracking system were strictly constructed to mimic the real-world data collection and passing patterns. The simulated pollutant concentration data were derived from the CFD dispersion results and the USV position in Gazebo. These data were collected by a 'sonde driver' and then passed to the main tracking system through a ROS interface. This procedure was designed to simulate the behaviour of a multi-parameter sonde [26], [27], which is commonly used in marine environments to measure pollutant concentrations. Upon receiving the probed data from the 'sonde driver', the main algorithm, introduced in Section III, updates the estimation of the pollution source and calculates the navigation waypoint. This waypoint was sent to the ArduPilot also via a ROS interface, which eventually drove the thrusters of the USV.

It is also worth noting that the main source tracking algorithm was constructed as a ROS action server, which provides a ROS action. A ROS action, as described by Macenski et al. [28], enables convenient interaction with procedures that require a significant amount of time to return a response. It is widely applied in fields of path planning [29] and manipulation [30]. Constructing the main tracking algorithm as an action server also offers a means of extension for future modular development. Several action servers can be incorporated into a higher-level decision-making logic through behaviour trees [31] and state machines [32].

III. THE UNCERTAINTY-AWARE PROBABILISTIC TRACKING ALGORITHM

In the proposed tracking system, an uncertainty-aware estimate of the source location was iteratively updated; the update was based on the probed data passed from the sonde driver. As described in [33], the information about the estimation obtained in the next navigation waypoint can be quantified as the expected information gain. The navigation waypoint that maximises the expected information gain was selected and executed by ArduPilot. Throughout the source tracking procedure, the uncertainty levels of the estimates were closely monitored. When the uncertainty levels reached a satisfactory threshold, the server containing the tracking system would respond with the latest estimate as final results.

In line with several works in pollution survey [12], [20], [34], the tracking area was discretised into a set of equally sized grids g_i . Each grid was attached to a coordinate with respect to a local North, East, Up (NEU) frame, (x_i, y_i) , and the probability, $p(g_i)$, that the source of the pollution is contained within the grid was recorded. Therefore, the entire grid map was constructed into a discrete probability distribution, which represented the overall estimate of the

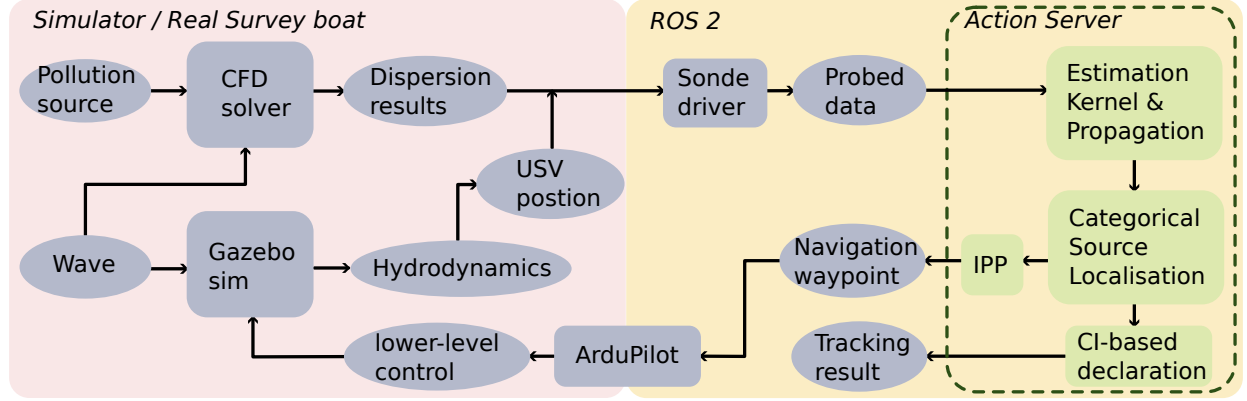


Fig. 2: Overall workflow of the proposed framework.

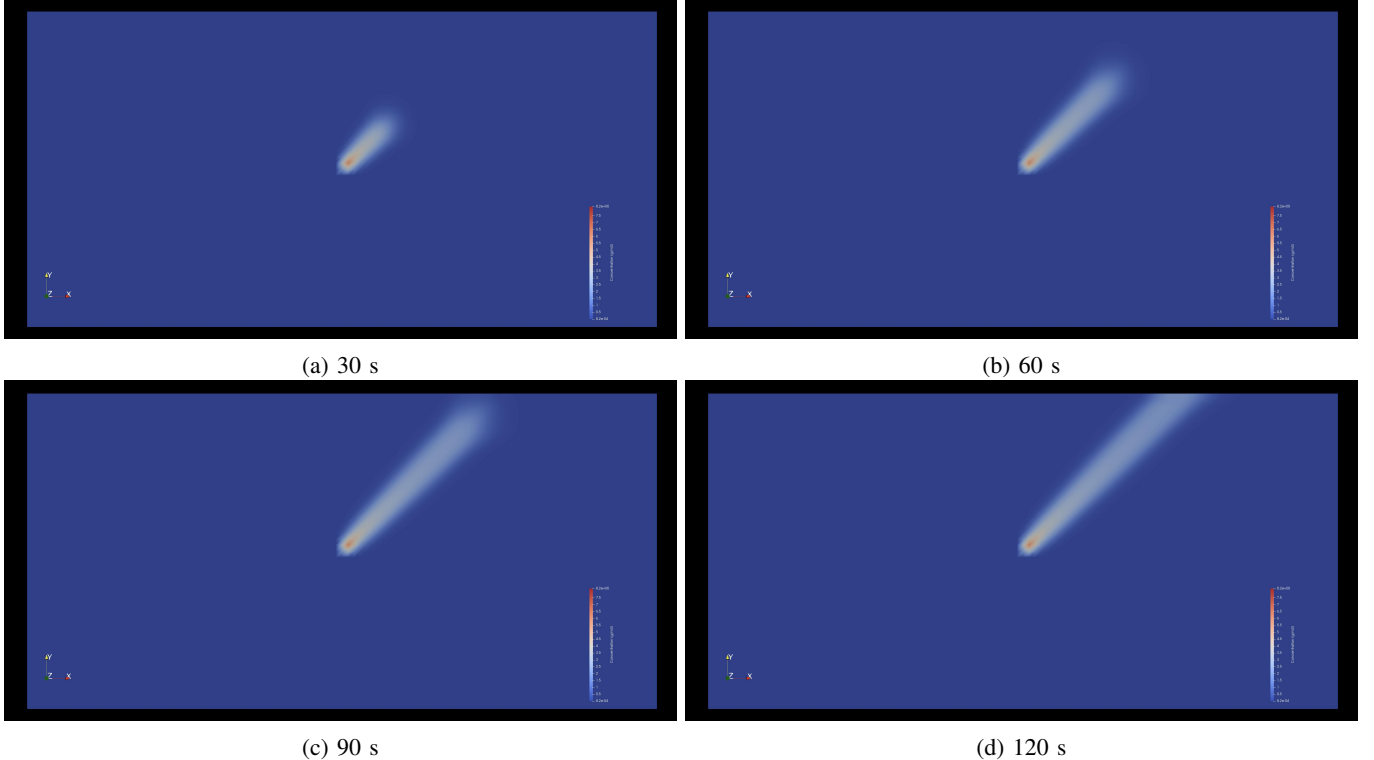


Fig. 3: The dispersing pollution plume simulated by the CFD solver.

pollution source location. Instead of formulating multivariate Bernoulli distributions [17], the grid map was formulated into a categorical distribution with k categories, where k is the number of grids. This addressed the ambiguity caused by normalising the multivariate Bernoulli and assuming the Bernoulli distributions as collectively independent. Using the categorical distribution, the best estimate was given as the expectation of it:

$$x_s = \sum_i x_i p(g_i) \quad (2)$$

$$y_s = \sum_i y_i p(g_i) \quad (3)$$

On receiving new probed data, a real-time estimate instance was generated using the method as proposed by Ojeda et al. [17]. In this method, a local estimate was obtained via Gaussian kernels:

$$p_t(g_i|z_t = 1) \sim \mathcal{N}\left(\frac{\mathbf{v}}{\|\mathbf{v}\|}, \sigma_a^2\right) \quad (4)$$

$$p_t(g_i|z_t = 0) \sim \mathcal{N}\left(\frac{\mathbf{r}}{\|\mathbf{r}\|}, \sigma_b^2\right) \quad (5)$$

where z_t is the probed data at time t ; $z_t = 1$ denotes an above-threshold measurement and $z_t = 0$ denotes a below-threshold measurement; \mathbf{r} is a vector pointing from the USV to the position of the latest above-threshold measurement; $\sigma_h^2 = 1$

and $\sigma_m^2 = 4$ are empirically selected variances. The local estimate covered only a small neighbourhood of the current grid, so the uncovered grids were assigned with the same probability as the closest grid that was covered by the local estimate. The existing estimate of the source location was then updated based on Bayes' theorem:

$$p(g_i|z_{1:t}) \propto p(g_i|z_t) p(g_i|z_{1:t-1}) \quad (6)$$

After the updated estimate of the pollution source location was obtained, a new navigation waypoint was selected to guide the USV cruising towards the next search area. Candidate waypoints were a set of grid centres of a defined neighbourhood encasing the current USV position. In this work, the workspace contained 100×50 grids, and the framework was run on a standard laptop with Intel® Core™ Ultra 7 Processor 155H and 32 GB RAM. The size of the neighbourhood was empirically selected as $11 \text{ grid} \times 11 \text{ grid}$ to balance the computational burden and the search horizon. Among all g_i within the neighbourhood, the candidate that maximises the expected information gain was selected as the next navigation waypoint. The information gain was formulated as the Kullback-Leibler Divergence (KLD) between the future and the existing estimate. Although the use of KLD as information gain was partially based on the existing works [17], [35], the probabilistic modelling was modified from a multivariate Bernoulli into a categorical distribution as mentioned previously. This modification utilised the correlation among the grids without assuming that they are collectively independent. The information gain derived from the categorical-distribution estimate was given as:

$$IG(g|p_{t-1}) = p_{t-1} \sum_{i=1}^k p_{t,a}(g_i) \ln \frac{p_{t,a}(g_i)}{p_{t-1}(g_i)} + (1 - p_{t-1}) \sum_{i=1}^k p_{t,b}(g_i) \ln \frac{p_{t,b}(g_i)}{p_{t-1}(g_i)} \quad (7)$$

where $p_{t,a}$ and $p_{t,b}$ are the future estimates of the source location given the above-threshold and below-threshold measurements, respectively.

In order to closely monitor the uncertainty level, a novel step was to use credible intervals of the source location to quantify the uncertainty level during the tracking. The credible interval $[q_l, q_u]$, is a Bayesian statistics concept [36], which is defined as that the source location has a probability γ to be within it:

$$\sum_{i=q_l}^{q_u} p(g_i|z_{1:t}) \geq \gamma \quad (8)$$

The γ -smallest credible interval [gls] was selected from various definitions. The Smallest Credible Interval (SCI) $[q'_l, q'_u]$ is defined as:

$$\begin{aligned} \forall [q_l, q_u] \in \left\{ [q_l, q_u] \mid \sum_{i=q_l}^{q_u} p(g_i|z_{1:t}) \geq \gamma \right\} \\ [q'_l, q'_u] = \arg \min_{[q_l, q_u]} (q_u - q_l) \end{aligned} \quad (9)$$

which facilitates a precise representation of the uncertainty level by focusing on the highest probability mass area. Besides providing a real-time representation of uncertainty levels, the SCI was also used to determine the termination condition of the tracking system. When $q'_u - q'_l \leq \tau$, where τ is the SCI threshold, the action server will respond to the request client with the latest best estimate of the pollution source location. The threshold for a 99%-SCI was given as the length of two grids in this work. The $\gamma = 99\%$ and the extremely small threshold value were selected based on the fact that the simulated environment is inevitably more ideal compared with reality, though high-fidelity simulation has been used. When this is applied to real USVs, we recommend suitable adjustments of these parameters.

IV. RESULTS

As outlined in the introduction, the objective of the proposed framework was to achieve uncertainty-aware autonomous pollution source tracking using a survey USV in the provided high-fidelity simulation environment. In this section, validations carried out within two simulated scenarios were presented.

Both of the simulated scenarios were configured within a $500 \text{ m} \times 250 \text{ m}$ workspace. As mentioned in III, the workspace was discretised into 100×50 equally spaced grids. The size of each individual grid was $5 \text{ m} \times 5 \text{ m}$. In the simulation, the origin of the local NEU frame used for localisation was attached to the centre of the workspace. We assumed the wave field was uniform within the workspace. This assumption is frequently adopted in the wave velocity measurement in practical situations [11], [37]. Therefore, the wave velocity was represented as a two-dimensional vector, $\mathbf{v} \in \mathbb{R}^2$. The simulated pollutant was selected as fluorescein, an organic dye, so the diffusion coefficient was configured as $\lambda = 4.9 \times 10^{-10}$ [38]. The two scenarios were devised with different source locations, wave velocities and starting positions of the survey USV. The configuration details can be found in Tab. I.

TABLE I: Configuration of the validation scenarios

Scenario	(a)	(b)
Source location (m)	(2.5, 2.5)	(102.5, -52.5)
Source release rate (kg/s)	2.5	2.5
USV starting position (m)	(120, 120)	(-120, 120)
Wave velocity (m/s)	$[1.2247, 1.2247]^T$	$[-1.2247, 1.2247]^T$

In both scenarios, the source tracking system successfully identified the pollution source without human intervention in most cases. Using the method described previously, the success of identification was controlled by the SCI of the estimated distribution. In these validations, the SCI threshold was $\tau = 10 \text{ m}$. For each scenario, three trials were conducted, and the source tracking results were given in Tab. II. Considering the resolution of the grid map was $5 \text{ m} \times 5 \text{ m}$, the mean errors reported in both scenarios were excellent. The detailed

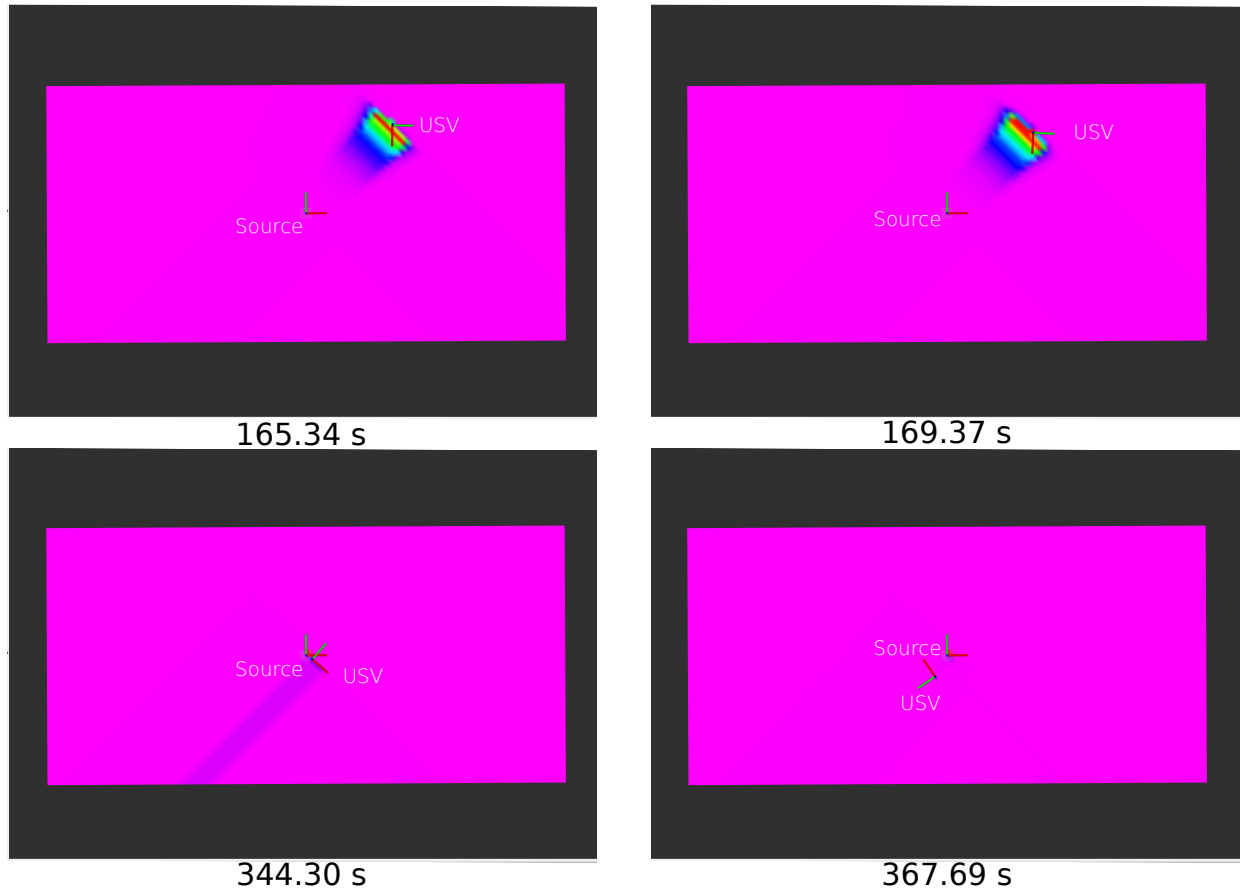
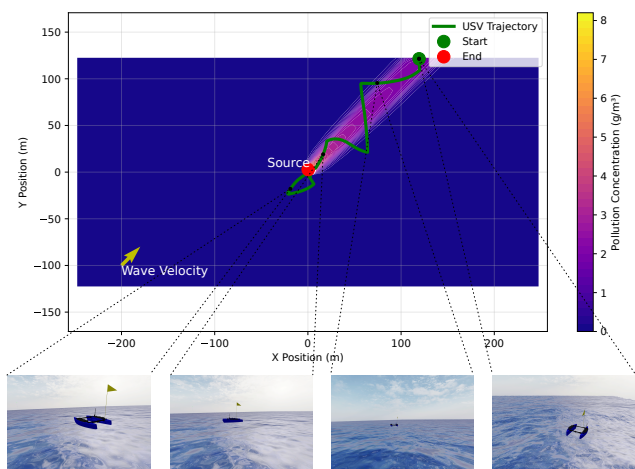
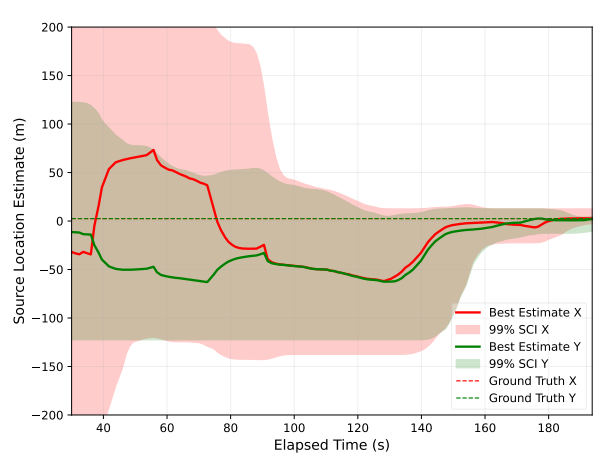


Fig. 4: Source location probability map at different time steps

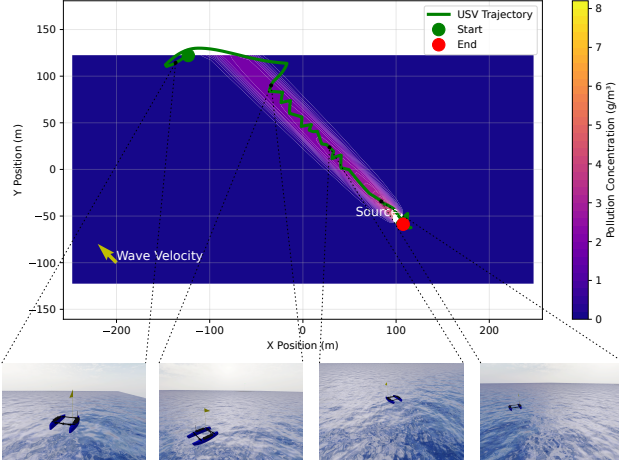


(a) Active tracking trajectory in simulated environment



(b) Source location estimate and SCI

Fig. 5: Scenario (a) of the validation. The source location is at (2.5 m, 2.5 m) and the USV starting position is at (120 m, 120 m).



(a) Active tracking trajectory in simulated environment



(b) Source location estimate and SCI

Fig. 6: Scenario (b) of the validation. The source location is at (102.5 m, -52.5 m) and the USV starting position is at (-120 m, 120 m).

data from one trial in each scenario were provided with their trajectory and uncertainty levels in Fig. 5 and 6.

TABLE II: Summary of the validation results

Scenario	(a)	(b)
mean error (m)	5.34	0.38
average runtime (s)	284.07	312.77
success rate (%)	100	66.67

At the beginning, the survey USV cruised along the pollutant plume. On the whole, it moved to the upwave direction, as shown in Fig. 5a and 6a. Towards the end, the survey USV overshot the pollution source, reaching an area with little pollutant. At this stage, the tracking system guided the USV to conduct a detailed search in the high probability mass area; an example of a series of source location probability maps is shown in Fig. 4. This detailed search typically included numerous re-entering and leaving the pollutant plume. The SCI noticeably dropped during this search, as can be seen in Fig. 5b and 6b, and eventually reached the 10 m threshold.

In scenario (b), the time consumed by the tracking system was extensively longer than in scenario (a). Although the Euclidean distance between the source and the USV starting point was slightly longer in scenario (b), the striking difference between the consumed times could be mainly attributed to the starting position of the survey USV; in scenario (b), the starting position was located outside the pollutant plume. It was recognised that, prior to tracking within the plume, the USV conducted a considerable amount of exploration to obtain the first non-trivial pollution concentration. This was unlike scenario (a), where non-trivial pollution concentration measurements were available at the start.

It should, however, be noted that if the USV starting position was exceptionally far away from the pollutant plume,

there would be a good probability that the tracking system failed to identify the source, for example, when the starting position was placed on the upwave direction with respect to the source. This was due to the tracking algorithm relying on above-threshold pollution concentration measurements to correct itself when the USV left the plume. The exploration procedure that discovered the initial non-trivial measurement was out of the scope of this article. Nevertheless, as suggested in II, an exploration action server can be easily integrated with the proposed framework using the behaviour tree in future work.

V. DISCUSSION AND CONCLUSION

Prior work has demonstrated the effectiveness of active tracking in pollution monitoring [20]. For example, Ojeda et al. [17] presented a method for indoor gas source localisation using Bayesian estimation and IPP, while Bayat et al. [19] reported a particle-filter-based active tracking system for marine pollution. However, a significant gap remains, as no existing work has validated such a system in a high-fidelity marine environment. To address this, this paper proposes an uncertainty-aware active pollution source tracking framework based on Bayesian estimation. We validate the proposed system in a high-fidelity, ROS-compatible simulation environment across various scenarios, demonstrating its reliable performance.

The proposed framework makes several key contributions. While our tracking system is structurally analogous to the method of Ojeda et al. [17], we have improved the underlying probability model to eliminate numerical ambiguities. Furthermore, this work extends the findings of Bayat et al. [19] by developing a more comprehensive Bayesian-based active tracking system and validating it in a significantly higher-fidelity environment. To our knowledge, this is the first framework to achieve active pollution source tracking

validated in a high-fidelity marine environment. The robust performance demonstrated in these validations supports its potential for future hardware implementation.

This work has several limitations that point to future research directions. Currently, the framework is limited to the source tracking function; incorporating an exploration module would be beneficial to ensure initial, above-threshold measurements can be reliably obtained. Finally, while the simulator was constructed in high fidelity to serve as a strong proof of concept, future work will involve real-world hardware implementation to validate the framework's performance on a physical system.

REFERENCES

- [1] E. L. Johnston, M. Mayer-Pinto, and T. P. Crowe, "REVIEW: Chemical contaminant effects on marine ecosystem functioning," *Journal of Applied Ecology*, vol. 52, no. 1, pp. 140–149, 2015, _eprint: <https://besjournals.onlinelibrary.wiley.com/doi/pdf/10.1111/1365-2664.12355>. [Online]. Available: <https://onlinelibrary.wiley.com/doi/abs/10.1111/1365-2664.12355>
- [2] V. Tornero and G. Hanke, "Chemical contaminants entering the marine environment from sea-based sources: A review with a focus on European seas," *Marine Pollution Bulletin*, vol. 112, no. 1, pp. 17–38, Nov. 2016. [Online]. Available: <https://www.sciencedirect.com/science/article/pii/S0025326X16304957>
- [3] P. J. Landrigan, J. J. Stegeman, L. E. Fleming, D. Allemand, D. M. Anderson, L. C. Backer, F. Brucker-Davis, N. Chevalier, L. Corra, D. Czerucka, M.-Y. D. Bottein, B. Demeneix, M. Depledge, D. D. Deheyn, C. J. Dorman, P. Fénichel, S. Fisher, F. Gaill, F. Galgani, W. H. Gaze, L. Giuliano, P. Grandjean, M. E. Hahn, A. Hamdoun, P. Hess, B. Judson, A. Laborde, J. McGlade, J. Mu, A. Mustapha, M. Neira, R. T. Noble, M. L. Pedrotti, C. Reddy, J. Rocklöv, U. M. Scharler, H. Shanmugam, G. Taghian, J. A. van de Water, L. Vezzulli, P. Weihe, A. Zeka, H. Raps, and P. Rampal, "Human Health and Ocean Pollution," *Annals of Global Health*, vol. 86, no. 1, p. 151, Dec. 2020. [Online]. Available: <https://www.ncbi.nlm.nih.gov/pmc/articles/PMC7731724/>
- [4] J. C. Biswas, M. M. Haque, M. Maniruzzaman, and N. Kalra, "Coastal and Marine Pollution in Bangladesh: Pathways, Hotspots and Adaptation Strategies," *European Journal of Environment and Earth Sciences*, vol. 2, no. 4, pp. 26–34, Jul. 2021. [Online]. Available: <https://www.ej-geo.org/index.php/ejgeo/article/view/133>
- [5] A. H. S. Solberg, "Remote Sensing of Ocean Oil-Spill Pollution," *Proceedings of the IEEE*, vol. 100, no. 10, pp. 2931–2945, Oct. 2012, conference Name: Proceedings of the IEEE. [Online]. Available: <https://ieeexplore.ieee.org/document/6235983>
- [6] G. Brantner and O. Khatib, "Controlling Ocean One: Human–robot collaboration for deep-sea manipulation," *Journal of Field Robotics*, vol. 38, no. 1, pp. 28–51, 2021, _eprint: <https://onlinelibrary.wiley.com/doi/pdf/10.1002/rob.21960>. [Online]. Available: <https://onlinelibrary.wiley.com/doi/abs/10.1002/rob.21960>
- [7] M. Trincavelli, M. Reggente, S. Coradeschi, A. Loutfi, H. Ishida, and A. J. Lilienthal, "Towards environmental monitoring with mobile robots," in *2008 IEEE/RSJ International Conference on Intelligent Robots and Systems*, Sep. 2008, pp. 2210–2215, iSSN: 2153-0866. [Online]. Available: <https://ieeexplore.ieee.org/abstract/document/4650755>
- [8] F. Fahimi, "Autonomous Surface Vessels," in *Autonomous Robots: Modeling, Path Planning, and Control*, F. Fahimi, Ed. Boston, MA: Springer US, 2009, pp. 1–42. [Online]. Available: https://doi.org/10.1007/978-0-387-09538-7_7
- [9] T. Jing, Q.-H. Meng, and H. Ishida, "Recent Progress and Trend of Robot Odor Source Localization," *IEEE Transactions on Electrical and Electronic Engineering*, vol. 16, no. 7, pp. 938–953, 2021, _eprint: <https://onlinelibrary.wiley.com/doi/pdf/10.1002/tee.23364>. [Online]. Available: <https://onlinelibrary.wiley.com/doi/abs/10.1002/tee.23364>
- [10] S. Pang and J. Farrell, "Chemical Plume Source Localization," *IEEE Transactions on Systems, Man, and Cybernetics, Part B (Cybernetics)*, vol. 36, no. 5, pp. 1068–1080, Oct. 2006. [Online]. Available: <https://ieeexplore.ieee.org/abstract/document/1703649>
- [11] M. Hutchinson, C. Liu, and W.-H. Chen, "Source term estimation of a hazardous airborne release using an unmanned aerial vehicle," *Journal of Field Robotics*, vol. 36, no. 4, pp. 797–817, 2019, _eprint: <https://onlinelibrary.wiley.com/doi/pdf/10.1002/rob.21844>. [Online]. Available: <https://onlinelibrary.wiley.com/doi/abs/10.1002/rob.21844>
- [12] Y. Liu, C. M. Harvey, F. E. Hamlyn, and C. Liu, "Bayesian estimation and reconstruction of marine surface contaminant dispersion," *Science of The Total Environment*, vol. 907, p. 167973, Jan. 2024. [Online]. Available: <https://www.sciencedirect.com/science/article/pii/S0048969723066007>
- [13] W. Chen and L. Liu, "Pareto Monte Carlo Tree Search for Multi-Objective Informative Planning," in *Proceedings of Robotics: Science and Systems*, vol. XV, FreiburgimBreisgau, German, Jun. 2019, p. 72. [Online]. Available: <https://www.roboticsproceedings.org/rss15/p72.html>
- [14] D. Fox, W. Burgard, and S. Thrun, "Active Markov localization for mobile robots," *Robotics and Autonomous Systems*, vol. 25, no. 3, pp. 195–207, Nov. 1998. [Online]. Available: <https://www.sciencedirect.com/science/article/pii/S0921889098000499>
- [15] J. A. Placed, J. Strader, H. Carrillo, N. Atanasov, V. Indelman, L. Carlone, and J. A. Castellanos, "A Survey on Active Simultaneous Localization and Mapping: State of the Art and New Frontiers," *IEEE Transactions on Robotics*, pp. 1–20, 2023.
- [16] H. Zhu, J. J. Chung, N. R. Lawrence, R. Siegwart, and J. Alonso-Mora, "Online Informative Path Planning for Active Information Gathering of a 3D Surface," in *2021 IEEE International Conference on Robotics and Automation (ICRA)*, May 2021, pp. 1488–1494, iSSN: 2577-087X.
- [17] P. Ojeda, J. Monroy, and J. Gonzalez-Jimenez, "Information-Driven Gas Source Localization Exploiting Gas and Wind Local Measurements for Autonomous Mobile Robots," *IEEE Robotics and Automation Letters*, vol. 6, no. 2, pp. 1320–1326, Apr. 2021. [Online]. Available: <https://ieeexplore.ieee.org/document/9347683>
- [18] C. Rhodes, C. Liu, and W.-H. Chen, "Autonomous Source Term Estimation in Unknown Environments: From a Dual Control Concept to UAV Deployment," *IEEE Robotics and Automation Letters*, vol. 7, no. 2, pp. 2274–2281, Apr. 2022, conference Name: IEEE Robotics and Automation Letters.
- [19] B. Bayat, N. Crasta, H. Li, and A. Ijspeert, "Optimal search strategies for pollutant source localization," in *2016 IEEE/RSJ International Conference on Intelligent Robots and Systems (IROS)*, Oct. 2016, pp. 1801–1807, iSSN: 2153-0866. [Online]. Available: <https://ieeexplore.ieee.org/abstract/document/7759287>
- [20] S. Ma, C. Liu, C. M. Harvey, R. Bucknall, and Y. Liu, "Adaptive informative path planning for active reconstruction of spatio-temporal water pollution dispersion using Unmanned Surface Vehicles," *Applied Ocean Research*, vol. 156, p. 104458, Mar. 2025. [Online]. Available: <https://www.sciencedirect.com/science/article/pii/S014111872500046X>
- [21] B. Choy and D. D. Reible, "Advection-diffusion models," in *Diffusion Models of Environmental Transport*. CRC Press, 2000, num Pages: 10.
- [22] S. Ulfah, S. A. Awalludin, and Wahidin, "Advection-diffusion model for the simulation of air pollution distribution from a point source emission," *Journal of Physics: Conference Series*, vol. 948, no. 1, p. 012067, Jan. 2018, publisher: IOP Publishing. [Online]. Available: <https://dx.doi.org/10.1088/1742-6596/948/1/012067>
- [23] H. Jasak, A. Jemcov, and Z. Tuković, "OpenFOAM: A C++ Library for Complex Physics Simulations," in *Proceedings of the International Workshop on Coupled Methods in Numerical Dynamics*. Fakultet strojarstva i brodogradnje Sveučilišta u Zagrebu, 2007, pp. 47–66. [Online]. Available: <https://www.croris.hr/crosbi/publikacija/prilog-skup/538019>
- [24] R. Mainwaring, "Wave Sim," Jan. 2025. [Online]. Available: https://github.com/srmainwaring/asv_wave_sim
- [25] "ArduPilot," Jul. 2025. [Online]. Available: <https://ardupilot.org/>
- [26] S. Ma, "at_sonde_ros_driver," London, May 2025. [Online]. Available: https://github.com/ma-shangao/at_sonde_ros_driver
- [27] A. Q. Li, "ysi_exo," Jun. 2022. [Online]. Available: https://github.com/dartmouthrobotics/ysi_exo
- [28] S. Macenski, T. Foote, B. Gerkey, C. Lalancette, and W. Woodall, "Robot Operating System 2: Design, architecture, and uses in the wild," *Science Robotics*, vol. 7, no. 66, p. eabm6074, May 2022, publisher: American Association for the Advancement of Science. [Online]. Available: <https://www.science.org/doi/10.1126/scirobotics.abm6074>
- [29] S. Macenski, F. Martín, R. White, and J. G. Clavero, "The Marathon 2: A Navigation System," in *2020 IEEE/RSJ International Conference on Intelligent Robots and Systems (IROS)*, Oct.

- 2020, pp. 2718–2725, iSSN: 2153-0866. [Online]. Available: <https://ieeexplore.ieee.org/document/9341207>
- [30] M. Görner, R. Haschke, H. Ritter, and J. Zhang, “MoveIt! Task Constructor for Task-Level Motion Planning,” in *2019 International Conference on Robotics and Automation (ICRA)*, May 2019, pp. 190–196, iSSN: 2577-087X. [Online]. Available: <https://ieeexplore.ieee.org/abstract/document/8793898/authors>
- [31] M. Colledanchise and P. Ögren, “Behavior Trees and Automated Planning,” in *Behavior Trees in Robotics and AI*. CRC Press, 2018, num Pages: 44.
- [32] M. Foukarakis, A. Leonidis, M. Antona, and C. Stephanidis, “Combining Finite State Machine and Decision-Making Tools for Adaptable Robot Behavior,” in *Universal Access in Human-Computer Interaction. Aging and Assistive Environments*, C. Stephanidis and M. Antona, Eds. Cham: Springer International Publishing, 2014, pp. 625–635.
- [33] M. Vergassola, E. Villermaux, and B. I. Shraiman, “‘Infotaxis’ as a strategy for searching without gradients,” *Nature*, vol. 445, no. 7126, pp. 406–409, Jan. 2007, publisher: Nature Publishing Group. [Online]. Available: <https://www.nature.com/articles/nature05464>
- [34] J. Song and M. E. J. Stettler, “A novel multi-pollutant space-time learning network for air pollution inference,” *Science of The Total Environment*, vol. 811, p. 152254, Mar. 2022. [Online]. Available: <https://www.sciencedirect.com/science/article/pii/S0048969721073307>
- [35] A. O. Lopes and J. K. Mengue, “On information gain, Kullback-Leibler divergence, entropy production and the involution kernel,” *Discrete and Continuous Dynamical Systems*, vol. 42, no. 7, pp. 3593–3627, Jul. 2022, publisher: Discrete and Continuous Dynamical Systems. [Online]. Available: <https://www.aims.science.org/en/article/doi/10.3934/dcds.2022026>
- [36] L. E. Eberly and G. Casella, “Estimating Bayesian credible intervals,” *Journal of Statistical Planning and Inference*, vol. 112, no. 1, pp. 115–132, Mar. 2003. [Online]. Available: <https://www.sciencedirect.com/science/article/pii/S0378375802003270>
- [37] M. Cao, H. Bie, and X. Hu, “Behavior Composition for Marine Pollution Source Localization Using a Mobile Sensor Network,” *Applied Sciences*, vol. 12, no. 12, p. 5767, Jan. 2022, publisher: Multidisciplinary Digital Publishing Institute. [Online]. Available: <https://www.mdpi.com/2076-3417/12/12/5767>
- [38] S. A. Rani, B. Pitts, and P. S. Stewart, “Rapid Diffusion of Fluorescent Tracers into *Staphylococcus epidermidis* Biofilms Visualized by Time Lapse Microscopy,” *Antimicrobial Agents and Chemotherapy*, vol. 49, no. 2, pp. 728–732, Feb. 2005. [Online]. Available: <https://www.ncbi.nlm.nih.gov/pmc/articles/PMC547266/>